MOX-Report No. 33/2026

Integrating Environmental Control and Hyperspectral Imaging to Assess Light and Nutrient Effects on Lettuce Post-Harvest Quality in Vertical Farming

Franzoni, G.; Mirabella, S.; Dabek, A.; Ferro, N.; Antona, A.; Carlessi, M.; Cinquemani, S.; Matteucci, M.; Cocetta, G.; Perotto, S.

MOX, Dipartimento di Matematica
Politecnico di Milano, Via Bonardi 9 - 20133 Milano (Italy)

mox-dmat@polimi.it https://mox.polimi.it

Integrating Environmental Control and Hyperspectral Imaging to Assess Light and Nutrient Effects on Lettuce Post-Harvest Quality in Vertical Farming

Giulia Franzoni[1,8], Susanna Mirabella[2], Aleksander Dabek[3], Nicola Ferro[4], Alessandro Antona[6], Martina Carlessi[6], Simone Cinquemani[3], Matteo Matteucci[5], Giacomo Cocetta[7], Simona Perotto[2]

April 10, 2026

[1]Department of Earth and Environmental Sciences (DSTA), University of Pavia, Corso Strada Nuova, 65 - 27100 Pavia - Italy
[2]MOX-Department of Mathematics, Politecnico di Milano, Piazza Leonardo da Vinci 32, I-20133, Milano, Italy
[3]Department of Mechanical Engineering, Politecnico di Milano, Via privata Giuseppe La Masa, 1 20156, Milano, Italy
[4]Department of Molecular Sciences and Nanosystems, Ca' Foscari University of Venice, Campus Scientifico, Via Torino 155, 30170, Venezia Mestre, Italy
[5]Department of Electronics, Information and Bioengineering, Politecnico di Milano, Piazza Leonardo da Vinci 32, I-20133, Milano, Italy
[6]Agricola Moderna, Via S. Pertini 26, 20066, Melzo, Italy
[7]Department of Agricultural and Environmental Sciences, University of Milan, Via Celoria 2 20133 Milano, Italy

{susanna.mirabella, simona.perotto}@polimi.it
{aleksander.dabek, simone.cinquemani, matteo.matteucci}@polimi.it
giulia.franzoni@unipv.it
giacomo.cocetta@unimi.it
nicola.ferro@unive.it
alessandro.antona@agricolamoderna.com
martina.carlessi@rina.org

Abstract

Vertical farming offers an opportunity to optimize crop yield and quality through precise control of environmental factors. In this study, we investigated the effects of light spectrum composition and nutrient solution electrical conductivity (EC) on yield and on biochemical traits of lettuce (*Lactuca sativa L.* cv. Lollo Rosso) grown in a vertical farm. The experimental design combined three light treatments (high blue, low blue, and variable blue ratio) with three nutrient solution EC levels (1, 2, and 3 $dS \cdot m^{-1}$), resulting in nine treatment conditions. Plants were harvested

twice, and destructive analyses were conducted at harvest time and after 14 days of cold storage to assess yield, water content, pigments, sugars, nitrates, anthocyanins, phenolics, and electrolyte leakage.

Results showed that lettuce growth and quality were influenced by both nutrient solution composition and light spectrum: higher salt concentration enhanced growth but not yield, while blue light promoted plant compactness. Diluted solutions increased secondary metabolites under mild nutrient stress, with limited effects on pigment content, sugar dynamics, and postharvest preservation. As a complementary analysis, hyperspectral imaging (400–1000 nm) was applied to lettuce leaves. Spectral data were analysed using machine learning models to investigate the relationship between changes in reflectance and in chemical composition, by comparing leaves at harvest with those after 14 days of cold storage. The adopted approach demonstrated the feasibility of using hyperspectral imaging to classify lettuce leaves at different post-harvest stages and identified candidate combinations of spectral indices capable of capturing the degradation of specific chemical traits occurring during the storage period. Overall, this study highlights the central role of nutrient solution concentration and light spectrum in determining lettuce yield and quality in vertical farming, while demonstrating the added value of hyperspectral imaging as a supplementary approach for trait assessment.

1 Introduction

The intensification of agriculture through vertical farming is increasingly viewed as a viable response to rising demands for fresh, high-quality produce. By providing fully controlled growing conditions, vertical farms can deliver consistent yields, optimize resource use, and ensure year-round availability of crops. Lettuce is particularly suited to these systems due to its short production cycle, high economic value, and sensitivity to environmental inputs, making it a model crop for testing strategies to improve both yield and quality [1].

Within vertical farming systems, two factors are particularly important, namely light spectrum composition and nutrient solution concentration [1]. Light not only drives photosynthesis but also regulates morphology and the biosynthesis of pigments and secondary metabolites. In particular, the ratio of blue to red light has been shown to affect leaf structure, chlorophyll and carotenoid content, and stress-related compounds such as anthocyanins and phenolics [2]. Meanwhile, the electrical conductivity (EC) of the nutrient solution directly influences nutrient uptake, growth rate, and the accumulation of compounds such as nitrates and sugars. Both excessive and insufficient nutrient availability can impair crop performance. Thus, optimizing and monitoring light quality and EC is a key issue to maximizing resource efficiency and product quality, since the mutual interaction ultimately guides the fine-tuning of cultivation strategies in vertical farming [3].

In this study, we examine how different light spectra and nutrient solution concentrations affect lettuce yield in terms of biochemical traits including pigments, sugars, nitrates, and secondary metabolites. More specifically, the experiment, described in detail in Section 2.1, consisted in analysing the combination of three different light con-

ditions, varying the emission spectrum of the LED lamps, and three levels of electrical conductivity. The effect of the different growth condition was analysed both right after the harvest and after 14 days of cold storage.
As a complementary step, we investigated whether leaf-level hyperspectral imaging combined with machine learning analysis can improve our understanding of post-harvest variation in chemical traits, exploiting the ability of hyperspectral imaging to capture subtle reflectance differences that correlate with underlying biochemical composition [4, 5].

By integrating physiological and biochemical measurements with non-destructive hyperspectral imaging, this study shows that nutrient solution concentration and light spectrum are relevant drivers of lettuce yield and quality in vertical farming, and that hyperspectral data provide a valuable complementary tool for trait assessment and optimization.

2 Material and Methods

This section describes the experimental setup, crop management, and sampling procedures, followed by the analytical protocols and data-processing workflows used for laboratory and hyperspectral measurements.

2.1 Experimental setup and crop management

The trial was conducted on lettuce *Lactuca sativa L. cv. Lollo Rosso* in the vertical farm Agricola Moderna, located close to Milan, Italy. Lettuce seeds were sown in growing trays filled with peat. After an initial irrigation with water, the trays were placed in a germination chamber for three days under dark conditions and high relative humidity (100%). Once seedling emergence was complete, the trays were transferred to the vertical farm and placed on separate growth levels of an ebb-and-flow recirculating hydroponic system. Fifteen days after sowing, the lettuce seedlings were manually transplanted into new growth trays containing a larger volume of substrate (210 cc per pot).
The experimental design included 9 growth conditions obtained by varying both light spectral quality and nutrient solution concentration.
We tested three lighting treatments by adjusting the LED emission spectrum in terms of the red-to-blue (R:B) photon flux ratio: (i) a high-blue treatment (R:B = 3), (ii) a low-blue treatment (R:B = 6.5), and (iii) a dynamic treatment in which plants were grown under low blue during development and shifted to high blue close to harvest. The total light intensity was kept the same for all treatments.
The nutrient solutions were prepared by diluting a commercial concentrated stock solution to obtain three levels of electrical conductivity (EC): (1) EC = 1 $dS\,m^{-1}$, (2) EC = 2 $dS\,m^{-1}$, and (3) EC = 3 $dS\,m^{-1}$. The molar ratios of the administered nutrient solutions remained the same across the three levels of dilution. The experiment consisted of nine treatment combinations (three light spectra × three EC levels), each replicated four times. The pH, EC, and water temperature were measured before each irrigation using

a Bluelab Combo Meter (Bluelab Corporation Limited, Tauranga, New Zealand). The pH was maintained between 5.5 and 6.5 by periodically adding sulfuric acid. Water temperature was kept as close as possible to the ambient temperature [1]) to prevent thermal shock. Hydrogen peroxide was used to disinfect materials and in the nutrient solution. Temperature and relative humidity were maintained within optimal ranges for lettuce growth, and CO2 concentration was approximately 800ppm. Ventilation was adjusted to ensure uniform airflow across all experimental units. Light intensity and photoperiod were set based on prior experiments conducted by the company. The emission spectrum was modified according to the experimental scheme.

2.2 Data collection

Harvest was performed twice. The first harvest took place when plants reached an average height of 13 cm, measured from the collar. For each of the 9 growing conditions, mean plant height was computed independently and used as the harvest criterion. Therefore, harvest time could differ among treatments. To ensure high uniformity, plants were mechanically cut while leaving the collar intact.
Yield was recorded immediately as fresh weight (g per tray), and the growing cycle length was expressed as the number of days required for each growing treatment to reach the target height of 13 cm. Right after cutting, plant material was subsampled for laboratory analyses and hyperspectral image acquisition. In particular, for each growing condition, 18 plants were collected at the first harvest: 9 plants were analyzed immediately and 9 plants were placed in polypropylene bags and stored in the dark at 8 °C for 14 days (shelf-life test). In both the immediately-analyzed and stored subsets, 4 plants were used for laboratory determinations of dry weight, water content, chlorophylls, carotenoids, phenolic index, total anthocyanins, nitrates, total sugars, reducing sugars, sucrose, and electrolyte leakage. In addition, during the storage the CO_2 concentration inside the packages was also measured[2]. The remaining 5 plants were used for hyperspectral data acquisition.

After the first harvest, trays were returned to the vertical farm to allow regrowth. The nutrient solution was replaced with a fresh one and the same procedure adopted during the first cultivation phase was employed. A second harvest was carried out when plants again reached 13 cm and samples were collected for laboratory analyses. However, hyperspectral images were not acquired and no shelf-life test was performed on these samples.

[1] Measurements of pH, water temperature and EC were performed before each irrigation using a Bluelab Combo Meter (Bluelab Corporation Limited, Tauranga, New Zealand https://bluelab.com/products/bluelab-combo-meter

[2] This measurement was carried out through a Witt OXYBABY gas analyser (WITT-Gasetechnik, Witten, Germany) https://www.wittgas.com/us/products/gas-analyzers/ at day 7 and 14

2.2.1 Laboratory measurements

Laboratory analyses were conducted to quantify biomass and quality attributes of lettuce leaves. The protocols reported below describe sample preparation, instrumental measurements, and calculations used for data expression.

Dry weight and water content Approximately 10 g of fresh lettuce leaves (FW) were oven-dried at 65 °C until constant weight was reached. The dry weight (DW) was used to calculate the water content (WC) percentage

$$WC = 100 - \left(\frac{DW}{FW} \times 100\right).$$

Total chlorophylls and carotenoids Total chlorophyll (chlorophyll a + b) and carotenoids were extracted from lettuce leaves according to Lichtenthaler's method [6]. Leaf disc samples (30 mg), obtained with a 5 mm diameter cork borer, were placed into 15 mL tubes with 5 mL of 99.9% (v/v) methanol and kept in a dark room for 24 h at 4 °C. Afterwards, the solution was analysed using a spectrophotometer[3] and pigment concentrations were determined colorimetrically. Absorbance readings were measured at 665.2 and 652.4 nm for chlorophylls and 470 nm for total carotenoids. Pigment concentrations were calculated using Lichtenthaler's formulas.

Total sugars, reducing sugars, and sucrose The concentrations of total sugars, reducing sugars, and sucrose were determined from the same aqueous extract prepared for nitrate analysis. Total sugars were measured using the anthrone method with slight modifications [7]. The reagent was prepared by dissolving anthrone powder in 95% H_2SO_4 to obtain a concentration of 10.3 mM. The solution was stirred for 30–40 min to ensure complete dissolution of the powder. Subsequently, 0.5 mL of sample extract was added to 2.5 mL of anthrone reagent in 15 mL tubes and incubated on ice. After 5 min, the tubes were vigorously mixed and heated to 95 °C in a Dubnoff bath. Following a 10 min incubation, the tubes were cooled to room temperature, and absorbance readings at 620 nm were performed using the spectrophotometer. A calibration curve was generated using a glucose standard solution.
Reducing sugars were determined from the same extract using the dinitrosalicylic acid (DNS) method [8]. This colorimetric analysis is based on a redox reaction between 3,5-dinitrosalicylic acid and the reducing sugars in the sample extracts. The assay was performed by mixing 0.2 mL of plant extract with 0.2 mL of DNS in 2 mL tubes, followed by incubation at 100 °C in a Dubnoff bath for 5 min. After incubation, 1.5 mL of water was added to each sample. Once cooled to room temperature, the absorbance at 530 nm was measured using the spectrophotometer, with a glucose standard curve used for quantification.
The concentration of sucrose was determined from the same extract using the resorcinol

[3]Evolution 300 UV-Vis, Thermo Scientific, UK www.thermofisher.com

method [9]. The reagent mix was prepared by combining a 30% HCl solution, 8.75 mg of resorcinol, 22.5 mg of thiourea, 6.25 mL of glacial acetic acid, and 2.5 mL of deionized water. One hundred μL of extract and 100 μL of 2 N NaOH were added to a 2 mL tube, which was then placed in a Dubnoff bath at 100 °C for 10 min, with the shaker turned on. Subsequently, 750 μL of the reagent mix was added, and the tubes were returned to the Dubnoff bath at 80 °C for 10 min, with the shaker turned on. After incubation, the tubes were cooled to room temperature, and the absorbance of the extracts was measured using the spectrophotometer at 500 nm. The sucrose concentration in the samples was calculated by preparing a calibration curve with a sucrose standard solution.

Nitrate Approximately 1 g of lettuce leaves was homogenized in a mortar with 3 mL of water. The mixture was centrifuged at 4,000 rpm for 15 min at room temperature using a centrifuge[4]. The supernatant was separated and used for analytical determinations. The nitrate concentration in lettuce leaves was determined from the leaf extracts using a colorimetric method [10]. 20 μL of leaf extract were added to the bottom of a 15 mL tube, followed by 80 μL of 5% (w/v) salicylic acid in concentrated H_2SO_4. The tubes were rapidly shaken, and 3 mL of 1.5 N NaOH was added. The mixture was cooled to room temperature, and absorbance at 410 nm was measured using the spectrophotometer. Nitrate concentration was calculated using a KNO_3 standard curve.

Total anthocyanin and phenolic index Total phenols and anthocyanin were extracted from leaf disc samples (30 mg) obtained with a 5 mm diameter cork borer. Leaf discs were placed into 15 mL tubes with 3 mL of methanol acidified with HCl (1%) and kept in a dark room for 24 h at 4 °C. Afterwards, absorbance readings were measured at 320 nm for total phenols and at 535 nm for anthocyanin, using the spectrophotometer. Phenolic index was expressed as Abs_{320} nm g^{-1}. Anthocyanin concentrations were expressed as cyanidin-3-glucoside equivalents using the molar extinction coefficient, ε, of 29,600 L mol^{-1} cm^{-1} [11, 12].

Electrolyte leakage Three leaf discs, obtained using a 9 mm cork borer, were placed into a 50 mL tube containing 20 mL of distilled water. The samples were incubated at room temperature with continuous shaking for 2 h. The electrical conductivity of the solution was measured using a digital electrical conductivity meter[5] on the same samples after freezing at -20 °C and subsequent thawing. Electrolyte leakage was expressed as a percentage of the total electrolytes [13].

2.2.2 Hyperspectral image acquisition

Hyperspectral imaging was used to measure leaf reflectance for subsequent spectral analysis.

[4]ALC centrifuge, model PK130R https://www.rdapassoni.it/
[5]Delta OHM digital electrical conductivity meter, model HD 9213 www.deltaohm.com

Lettuce plants' reflectance was measured using a hyperspectral camera[6] acquiring images in the 400–1000 nm range with a uniform sampling interval of 5 nm (120 spectral bands). Hyperspectral image acquisition was conducted inside an insulated light box illuminated by three halogen lamps and five LED lights (Fig. 1). A white reference panel was included in each acquisition and positioned at the same height as the top surface of the samples. For each of the 9 growing conditions, measurements were collected from

Figure 1: Light box used for hyperspectral image collection.

5 individual plants by imaging 3–4 leaves per plant. To reduce sensor and background noise, a reference image of the acquisition area without a sample was obtained and used for correction. The resulting raw hyperspectral data, R_{sample}, were calibrated using the white reference signal, R_{white}, as $R_{\text{calibrated}} = R_{\text{sample}}/R_{\text{white}}$. Finally, leaf segmentation was performed using an unsupervised clustering approach based on spectral features. For each pixel, a reduced feature set was constructed consisting of reflectance at 550 nm, 680 nm, and 800 nm, corresponding to the green, red, and near-infrared spectral regions, respectively, together with the normalized difference vegetation index (NDVI) and the mean reflectance across all spectral bands. These features were used as input to a K-means clustering algorithm ($K = 3$) to partition the image into clusters corresponding to leaf tissue, background, and shadow. The cluster exhibiting the highest mean NDVI was identified as the leaf class. The resulting binary mask was subsequently refined using morphological operations to remove small artifacts, fill internal gaps, and smooth discontinuities (see Fig. 2).

2.3 Data analysis

The two complementary data streams in Sects. 2.2.1-2.2.2 were analyzed. The laboratory measurements were evaluated using inferential statistics to test treatment effects, whereas the hyperspectral reflectance data were analyzed exploiting machine-learning

[6]HERA IPERSPETTRALE - HERA VNIR (400-1000 nm) https://nireos.com/product/hera-vnir.

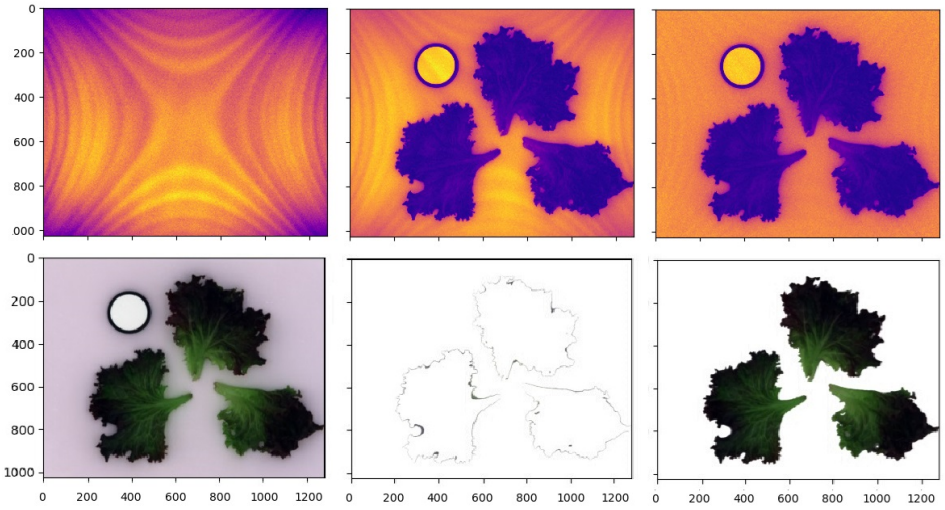

Figure 2: Preprocessing and leaf segmentation: hyperspectral images displayed by using spectral band 10 for visualization purposes (top row) – acquisition area without samples, showing background illumination artifacts from the light box (left), raw hyperspectral image with lettuce samples and the white reference circular disk (center), calibrated hyperspectral image after background correction and reflectance normalization using the white reference (right); RGB renderings (bottom row) – calibrated hyperspectral image (left), cluster corresponding to background and shadow regions (center), final leaf segmentation (right).

classification and correlation analyses to link spectral variation to postharvest changes. Laboratory measurements were analysed using GraphPad Prism 9, a statistics and graphing package widely used in the life sciences for data visualization, curve fitting, and standard statistical analyses. Differences were tested by two-way ANOVA with a significance threshold of $p < 0.05$. When significant effects were detected, means were compared using Tukey's post hoc test.

Hyperspectral data analysis focused on two objectives. First, we evaluated whether spectral reflectance could discriminate between leaves measured at harvest and after cold storage. For each of the 9 growing conditions, 5 hyperspectral images were acquired immediately after the first harvest and after 14 days of storage, resulting in 90 images in total. For each image, the mean reflectance spectrum was computed over leaf pixels after background removal. Spectra were then partitioned into training, validation, and test sets, and a classifier was trained using an XGBoost model. The validation set was used to select the best combination of spectral preprocessing and feature selection. The preprocessing methods compared were: no transformation (raw spectra), first derivative, second derivative, standard normal variate, normalization, and Savitzky–Golay first derivative filtering (Fig. 3). Feature selection strategies relying on using all spectral bands or reducing dimensionality by principal component analysis (10 or 20 principal components). Second, we investigated whether spectral changes between harvest and

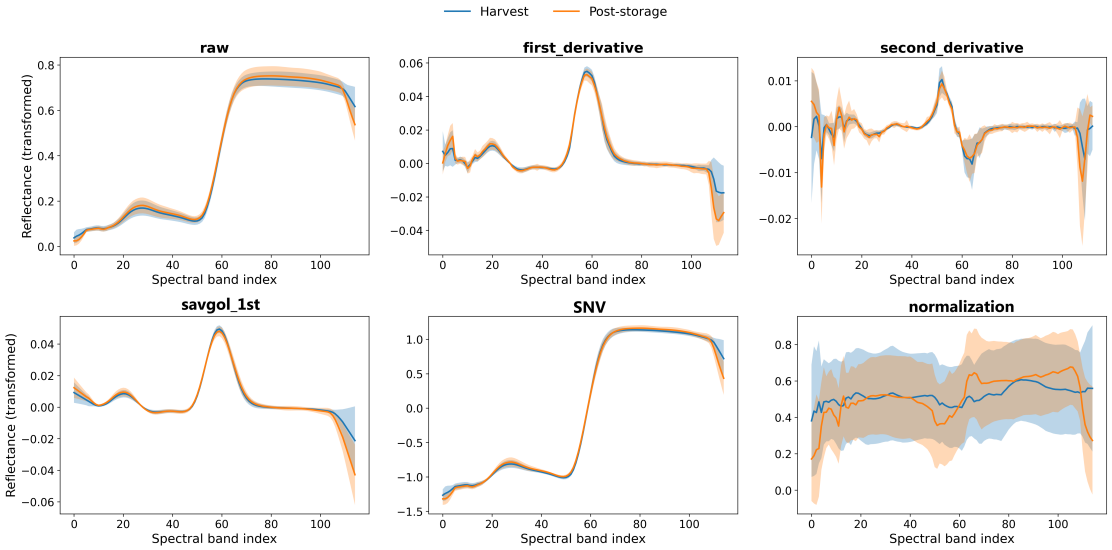

Figure 3: Spectral transformations tested to optimize classification performance: average reflectance spectra (± standard deviation) are shown for harvest (blue) and post-storage (orange) leaves, under 6 preprocessing methods: raw, first derivative, second derivative (top row, from left to right), Savitzky–Golay first derivative (savgol_1st), standard normal variate (SNV), and normalization.

post-storage stages were associated with changes in chemical traits. For each growing condition, spectra were averaged separately for harvest and stored samples, and their difference was computed as the Δ-spectrum. From each Δ-spectrum, a set of commonly used vegetation indices was calculated (NDVI, GNDVI, NDRE, PRI, PSRI, ARI1, MCARI, CIredge, BNDVI, mND705, NDWI970, and WBI [14, 15, 16, 17, 18, 19, 20, 21, 22, 23]). The spectral macro-bands (400–1000 nm) contributing to each index are summarised in Fig. 4. In parallel, chemical changes were computed as Δ-traits for each treatment and compound. Pearson correlation coefficients were then calculated for each index–trait pair across the 9 growing conditions.

3 Results and discussion

In this section, we present and discuss the main findings of the study. The results are organized into two parts: the outcomes of the laboratory measurements and the results of the hyperspectral data analysis.

3.1 Outcomes of the laboratory measurements

In this section, the results of the statistical analysis on the laboratory measurements are presented and discussed across harvests and post-storage samples. Treatment effects are

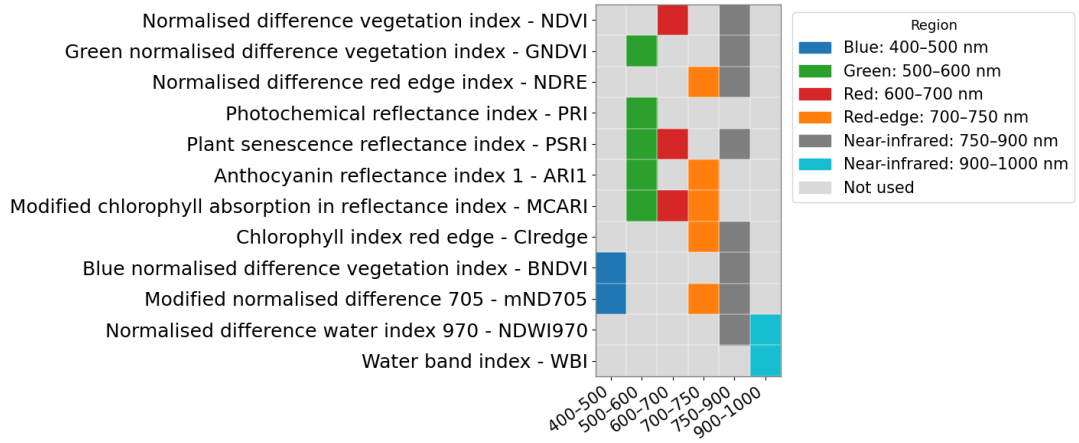

Figure 4: Spectral macro-bands used in the computation of vegetation indices. Columns represent 6 macro-bands, while rows correspond to the 12 selected vegetation indices. A colored square indicates that a given index incorporates reflectance from that spectral region.

reported for the main biomass, compositional, and physiological traits, highlighting the roles of nutrient-solution EC and light spectrum.

Yield and growing cycle duration EC provides an indirect estimate of nutrient availability and is therefore a key management lever in vertical farming, where both insufficient and excessive nutrient concentrations can constrain growth and productivity. In this context, we evaluated how EC level and blue-light proportion affected yield and crop timing. For confidentiality reasons related to the private company, yield and growing-cycle length are reported as percentage deviations from the overall mean (Tables 1 and 2, respectively). At the first harvest, the interaction between blue light proportion and nutrient-solution EC was not statistically significant, whereas both factors had significant main effects separately. In particular, the highest yields were observed at EC = 2 dS m^{-1}, particularly under high or variable blue light proportions, while yields at EC = 1 dS m^{-1} and EC = 3 dS m^{-1} were generally lower, especially when combined with variable or low blue light percentage.
In the second harvest, yield patterns further suggested that EC was the dominant driver under the tested conditions, while spectral composition modulated the response to a lesser extent. Specifically, plants grown at EC = 2 dS m^{-1} again achieved the highest yields, with both high and low blue light proportions, whereas the lowest yields consistently occurred at EC = 1 dS m^{-1} regardless of the percentage of blue light. Overall, these results indicate that EC = 2 dS m^{-1} provided the best performance, in agreement with previous works identifying EC optimization as critical for lettuce nutrient uptake and biomass production (see, e.g., [3]).

Growing-cycle duration varied across treatments and generally decreased as EC in-

Table 1: Percentage changes of each experimental configuration yield compared to the average across treatments for the first and the second harvest (top panel). Letters indicate significant differences between the combinations of light and EC according to Tukey's post-hoc test where treatments sharing at least one letter are not significantly different. Effects of electrical conductivity (EC), blue light proportion (% blue), and their interaction for each harvest through the two-way ANOVA testing (bottom panel). Significance levels are indicated as ns ($p > 0.05$) and *** ($p < 0.001$).

EC [dS m^{-1}]	% blue	first harvest	storage
1	high	-1.5 bc	-29.2 e
1	variable	-12.1 d	-26.4 e
1	low	-11.0 d	-20.7 de
2	high	13.3 a	24.6 a
2	variable	10.2 a	5.3 bc
2	low	5.6 ab	27.5 a
3	high	5.6 ab	23.4 ab
3	variable	-6.1 cd	-1.0 c
3	low	-4.0 cd	-3.6 cd
% blue combined with EC		ns	***
% blue		***	***
EC		***	***

creased, indicating faster growth under higher nutrient availability (Table 2). During the first cycle (transplant to first harvest), the longest duration occurred at EC = 1 dS m^{-1} under high blue light, whereas intermediate durations were observed for EC = 1 dS m^{-1} under variable or low blue light and for EC = 2 dS m^{-1} under high or variable blue light. The shortest first-cycle durations were recorded at EC = 3 dS m^{-1}, particularly with low or variable blue light proportions.

A comparable pattern was observed for the second cycle (first to second harvest), with slower regrowth at low EC and faster regrowth at higher EC. The acceleration at higher EC likely reflects enhanced nutrient supply and uptake, supporting the metabolic processes required to reach the target height. Conversely, the longer cycles at EC = 1 dS m^{-1} suggest suboptimal nutrition, which may slow cell division and elongation. Relative to EC, the effect of blue light proportion on cycle duration appeared secondary. High blue light tended to prolong the cycle under low EC, consistent with the known role of blue light in limiting elongation and promoting compact growth [2]. Under nutrient-rich conditions, the stimulatory effect of higher EC may partially offset the influence of blue light on growth rate. Overall, the fastest growth occurred under high EC combined with low or variable blue light, suggesting greater elongation when nutrient availability is not limiting. These results further indicate that light quality and EC can affect not only yield but also harvest timing, which is a key parameter for production planning [24].

Table 2: Percentage changes of each treatment growing cycle compared to the average across treatments for the transplant-first harvest and the first harvest-second harvest periods. Positive and negative variations indicate longer and shorter duration, respectively.

EC [dS m^{-1}]	% blue	transplant - first harvest	first harvest - second harvest
1	high	+22.2	+17.2
1	variable	+2.9	+17.2
1	low	+2.9	+17.2
2	high	+2.9	+3.1
2	variable	-3.5	-1.5
2	low	-3.5	-1.5
3	high	-3.5	-1.5
3	variable	-10.0	-25.0
3	low	-10.0	-25.0

Leaf water content A significant interaction between light spectrum and nutrient-solution EC was observed for water content percentage (Table 3). In particular, water content was generally lower at EC = 1 dS m^{-1} in the first harvest (94.1%), second harvest (92.5%), and after storage (93.9%) compared with higher EC levels. The lowest value was consistently recorded under the combination of EC = 1 dS m^{-1} and a high blue light proportion (93%), whereas plants grown at EC = 2 dS m^{-1} and EC = 3 dS m^{-1} generally showed higher water content. This pattern suggests a synergistic effect whereby limited nutrient availability at low EC may reduce water uptake (via changes in solution osmotic potential), and high blue light may further exacerbate water loss by promoting stomatal opening and transpiration [25]. Consistently, previous work has reported that non-optimal EC levels can decrease the water percentage in lettuce leaves [26].

Total chlorophylls and carotenoids The highest chlorophyll a+b concentration was observed under a low blue light percentage combined with high EC (EC = 3 dS m^{-1}), both at the first and second harvest (1.04 and 0.92 μg mg^{-1} FW, respectively). In contrast, the lowest values occurred under low blue light combined with EC = 2 dS m^{-1} or EC = 1 dS m^{-1} in the first and second harvest. After storage, chlorophyll a+b did not differ significantly among treatments, with an average value of approximately 0.79 μg mg^{-1} FW (Table 4). An increase in chlorophyll content with increasing nutrient-solution EC has been previously reported in lettuce [27] and in basil, kale, pepper, and tomato grown in either low EC–high pH or high EC–low pH (ideal hydroponic) solutions [28]. Although blue light is often associated with enhanced chlorophyll synthesis [29, 30], in the present study we observe an opposite trend, with higher chlorophyll levels observed under lower blue light proportions.

Table 3: Water content percentage in lettuce leaves after the first and second harvest, and after the storage (top panel). The data represent the average for each treatment ± the standard error. Letters indicate significant differences between the combinations of light and EC according to Tukey's post-hoc test where treatments sharing at least one letter are not significantly different. Effects of electrical conductivity (EC), blue light proportion (% blue), and their interaction for each harvest through the two-way ANOVA testing (bottom panel). Significance levels are indicated as ns ($p > 0.05$), ** ($p < 0.01$), and *** ($p < 0.001$).

EC [dS m^{-1}]	% blue	first harvest	second harvest	storage
1	high	93.4 ± 0.25 d	92.6 ± 0.19 c	92.9 ± 0.22 d
1	variable	94.3 ± 0.15 c	92.2 ± 0.03 c	94.5 ± 0.24 bc
1	low	94.6 ± 0.11 bc	92.8 ± 0.11 c	94.4 ± 0.15 c
2	high	95.3 ± 0.20 ab	94.1 ± 0.14 b	95.0 ± 0.29 abc
2	variable	95.3 ± 0.10 ab	94.5 ± 0.06 ab	95.5 ± 0.09 a
2	low	95.5 ± 0.16 a	94.6 ± 0.21 ab	95.3 ± 0.16 ab
3	high	95.1 ± 0.19 ab	94.8 ± 0.11 a	95.5 ± 0.03 a
3	variable	95.4 ± 0.13 a	94.8 ± 0.16 a	95.2 ± 0.17 abc
3	low	95.2 ± 0.16 ab	94.4 ± 0.07 ab	94.8 ± 0.09 abc
% blue combined with EC		**	**	***
% blue		**	ns	**
EC		***	***	***

Carotenoid concentrations followed a similar pattern. The highest values at both harvests were measured under low blue light combined with EC = 3 dS m^{-1}. At the first harvest, relatively high carotenoid levels were also observed under high blue light combined with EC = 3 dS m^{-1} and under variable blue light combined with EC = 2 dS m^{-1}. After storage, no significant differences among treatments were detected (Table 5). Because pigment concentrations can depend on cultivar [31], and because postharvest degradation is strongly driven by storage conditions (temperature, light exposure, humidity), the lack of treatment effects after storage suggests that pigment loss during storage was largely independent of the preharvest growing conditions.

Total sugars, reducing sugars, and sucrose Total sugar concentration was significantly affected by the interaction between nutrient-solution EC and blue light proportion at both the first and second harvest. At the first harvest, the highest total sugar levels (21.9 mg g^{-1} FW) were generally recorded at EC = 1 dS m^{-1}, regardless of blue light proportion, whereas values were approximately halved (10.5 mg g^{-1} FW) at EC = 2 dS m^{-1} and EC = 3 dS m^{-1} Fig. 5 A). The same overall pattern was observed at the second harvest, with higher total sugars at low EC, although the decline with increasing EC was more gradual. In particular, a steady decrease was evident under high blue light,

Table 4: Chlorophyll a+b (μg mg^{-1} FW) in lettuce leaves after the first and second harvest, and after the storage (top panel). The data represents the average for each treatment ± the standard error. Letters indicate significant differences between the combinations of light and EC according to Tukey's post-hoc test where treatments sharing at least one letter are not significantly different. Effects of electrical conductivity (EC), blue light proportion (% blue), and their interaction for each harvest through the two-way ANOVA testing (bottom panel). Significance levels are indicated as ns ($p > 0.05$) and * ($p < 0.05$).

EC [dS m^{-1}]	% blue	first harvest	second harvest	storage
1	high	0.76 ± 0.04 ab	0.75 ± 0.12 ab	0.83 ± 0.04
1	variable	0.76 ± 0.04 ab	0.51 ± 0.15 ab	0.75 ± 0.05
1	low	0.90 ± 0.07 ab	0.34 ± 0.09 b	0.79 ± 0.07
2	high	0.86 ± 0.09 ab	0.57 ± 0.09 ab	0.82 ± 0.12
2	variable	1.00 ± 0.11 ab	0.53 ± 0.05 ab	0.79 ± 0.04
2	low	0.60 ± 0.10 b	0.52 ± 0.17 ab	0.68 ± 0.11
3	high	0.95 ± 0.13 ab	0.75 ± 0.09 ab	0.73 ± 0.08
3	variable	0.88 ± 0.10 ab	0.62 ± 0.06 ab	0.69 ± 0.06
3	low	1.07 ± 0.04 a	0.92 ± 0.04 a	1.02 ± 0.06
% blue combined with EC		*	ns	ns
% blue		ns	ns	ns
EC		ns	*	ns

whereas values remained comparatively low and similar under low blue light (Fig. 5 B). After storage, total sugars did not differ significantly among treatments. However, the preharvest pattern was still visible, especially under low blue light, and the overall mean was 9.4 mg g^{-1} FW (Fig. 5 C).

Reducing sugars were significantly affected by EC, with higher concentrations at EC = 1 dS m^{-1} and lower concentrations at higher EC levels. This decrease was most pronounced at the first harvest, where reducing sugars declined from 34.1 mg g^{-1} FW (high blue light, EC = 1 dS m^{-1}) to 7.1 mg g^{-1} FW at EC = 2 dS m^{-1} (Fig. 6 A). In addition, reducing sugars tended to decrease as blue light proportion decreased (from high to low). Similar, but weaker, patterns were observed at the second harvest and after storage (Figs. 6 B,C).

Sucrose concentration was also significantly affected by EC. The highest sucrose levels were observed at EC = 1 dS m^{-1} under high blue light at the first harvest, second harvest, and after storage (Table 6).

Overall, these results indicate that sugar accumulation in lettuce was primarily driven by EC, with consistently higher total sugars, reducing sugars, and sucrose under low EC conditions. This agrees with previous findings in lettuce reporting a reduction in sugar concentration as EC increases [3, 32], which has been attributed to higher respiration

Table 5: Carotenoids (μg mg^{-1} FW) in lettuce leaves after the first and second harvest, and after storage (top panel). The data represents the average for each treatment ± the standard error. Letters indicate significant differences between the combinations of light and EC according to Tukey's post-hoc test where treatments sharing at least one letter are not significantly different. Effects of electrical conductivity (EC), blue light proportion (% blue), and their interaction for each harvest through the two-way ANOVA testing (bottom panel). Significance levels are indicated as ns ($p > 0.05$), * ($p < 0.05$) and ** ($p < 0.01$).

EC [dS m^{-1}]	% blue	first harvest	second harvest	storage
1	high	0.14 ± 0.01 ab	0.14 ± 0.02 ab	0.18 ± 0.02
1	variable	0.15 ± 0.01 ab	0.10 ± 0.03 ab	0.16 ± 0.01
1	low	0.17 ± 0.01 ab	0.07 ± 0.02 b	0.17 ± 0.01
2	high	0.17 ± 0.02 ab	0.11 ± 0.02 ab	0.16 ± 0.02
2	variable	0.20 ± 0.02 a	0.10 ± 0.01 ab	0.17 ± 0.01
2	low	0.12 ± 0.02 b	0.11 ± 0.03 ab	0.14 ± 0.02
3	high	0.19 ± 0.01 a	0.15 ± 0.02 ab	0.16 ± 0.01
3	variable	0.17 ± 0.02 ab	0.11 ± 0.01 ab	0.14 ± 0.01
3	low	0.20 ± 0.00 a	0.17 ± 0.01 a	0.20 ± 0.01
% blue combined with EC		**	ns	ns
% blue		ns	ns	ns
EC		*	*	ns

rates that reduce carbohydrate accumulation. The significant interaction with blue light proportion further suggests that light quality can modulate sugar levels, particularly under low nutrient availability. Other studies have reported different responses to spectral composition, including higher sucrose and starch under higher red light proportions [33] and increased hexose and sucrose accumulation when red light exceeds 50% [34]. These discrepancies support the view that carbohydrate metabolism in lettuce depends on both nutrient status and the Red:Blue lighting regime, including its temporal dynamics [29].

Nitrate Nitrate concentration was primarily driven by nutrient availability: EC had a significant effect, whereas blue light proportion did not (Fig. 7). This result is consistent with the established link between nitrogen supply and nitrate accumulation in leafy vegetables, where higher EC typically reflects greater nitrate input that can exceed the plant's assimilation capacity under nutrient-rich conditions [35, 3, 36, 32]. Accordingly, nitrate increased with EC at both harvests and after storage (opposite to the trend observed for sugars). At the first harvest, nitrate rose from approximately 683 mg kg^{-1} FW at EC = 1 dS m^{-1} to approximately 2661 mg kg^{-1} FW at EC = 3 dS m^{-1} (corresponding to a 289%, increase, Fig. 7 A). A similar response was observed at the second harvest, where nitrate at EC = 3 dS m^{-1} was almost 400% higher than at EC = 1 dS

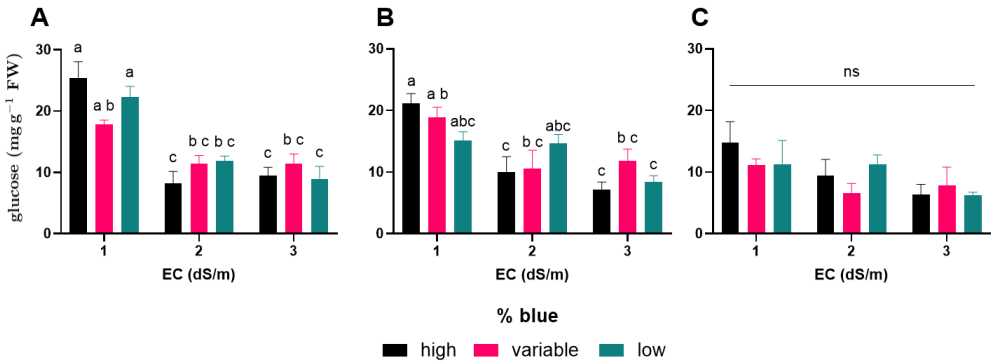

Figure 5: Total sugars (mg g^{-1} FW) in lettuce leaves after the first (A), second (B) harvest, and after the storage (C). The data represents the average for each treatment ± the standard error. Letters indicate significant differences between the combinations of light and EC according to Tukey's post-hoc test where treatments sharing at least one letter are not significantly different.

m^{-1} (Fig. 7 B). After storage, the same pattern persisted but was less pronounced, with nitrate values generally lower than immediately after harvest (Fig. 7 C), while EC = 2 dS m^{-1} consistently resulted in intermediate concentrations.
The absence of a significant blue light effect suggests that, under the present conditions, any light-quality influence on nitrate metabolism (e.g., via nitrate reductase activity) was secondary to the dominant role of nitrogen availability [37, 38]. Only a minor effect was observed at the first harvest for EC = 2 dS m^{-1}, with slightly lower nitrate under low blue light. From an applied perspective, these findings underscore the importance of EC management in hydroponic systems given consumer concerns and the current EU limits for nitrate in leafy vegetables (Commission Regulation No. 1258/2011). Notably, even at the highest EC tested, nitrate concentrations remained below the regulatory threshold.

Total anthocyanins and phenolic index nitrate (mg kg $^{-1}$ FW) Anthocyanin concentration showed different patterns at the first harvest, second harvest, and after storage (Table 7). A significant interaction between blue light proportion and EC was detected only at the first harvest. However, EC significantly affected anthocyanin at all sampling times. At the first harvest, the highest anthocyanin levels were measured at EC = 1 dS m^{-1}, particularly under high (34.8 Cyanidin eq. mg g^{-1} FW) or variable (40 Cyanidin eq. mg g^{-1} FW) blue light, suggesting that mild nutrient limitation at low EC may stimulate secondary-metabolite biosynthesis, including anthocyanins [39]. This response may be considered as a general stress-adaptation mechanism aimed at improving the antioxidant capacity of the plant. A comparable value was observed at EC = 3 dS m^{-1} under high blue light (36.6 Cyanidin eq. mg g^{-1} FW). At the second harvest and after storage, the maximum anthocyanin concentration again occurred under high blue light combined with EC = 1 dS m^{-1}, whereas other treatments showed lower

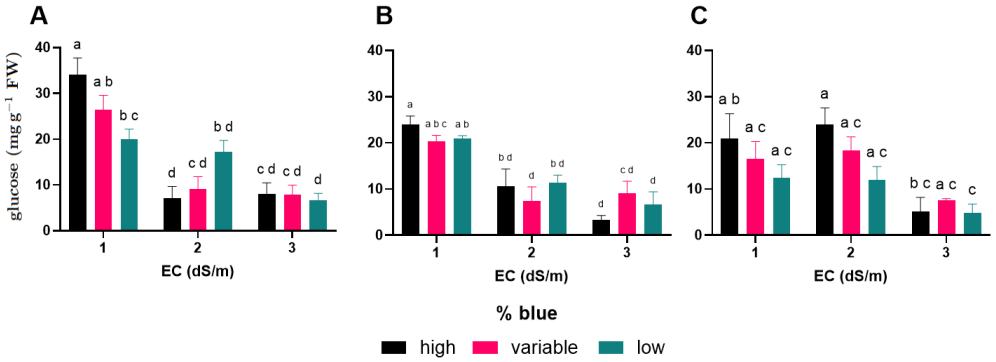

Figure 6: Reducing sugars (mg g^{-1} FW) in lettuce leaves after the first (A), second (B) harvest, and after the storage (C). The data represents the average for each treatment ± the standard error. Letters indicate significant differences between the combinations of light and EC according to Tukey's post-hoc test where treatments sharing at least one letter are not significantly different.

values. The lowest concentrations after storage were generally observed at EC = 3 dS m^{-1}, regardless of blue light proportion. The stimulatory role of blue light on flavonoid biosynthesis is well established [40], and the stronger response under low EC supports a synergistic effect of light quality and nutrient limitation on anthocyanin accumulation.

Total phenols were also influenced by the combined effects of blue light and EC, with a significant interaction at both the first and second harvest (Table 8). Consistent with the anthocyanin response, total phenols concentration was generally highest at EC = 1 dS m^{-1} under high or variable blue light, whereas the lowest values were associated with higher EC levels. This pattern supports the interpretation that low EC imposed a nutrient-stress condition that promoted secondary metabolism, and that blue light further enhanced phenolic accumulation, as reported previously [41]. The interaction was particularly evident at the second harvest, possibly reflecting cumulative effects across successive growth cycles.

Electrolyte leakage At the first harvest, electrolyte leakage (EL) was approximately 12% for most treatments, with the main exception being plants grown at EC = 3 dS m^{-1} under low blue light, which showed higher EL (16.9%) (Fig. 8 A). This response suggests reduced membrane stability under the combination of high EC and low blue light, potentially linked to higher ionic concentrations in tissues and a greater propensity for oxidative damage. Consistently, increased EL has been reported in lettuce under saline conditions [42, 43].

At the second harvest, EL responded differently to the combinations of EC and blue light. Under EC = 1 dS m^{-1}, EL increased as blue light proportion decreased, whereas plants grown under variable blue light showed similar EL values across EC levels (with a mean value of about 9.3%) (Fig. 8 B). This pattern may indicate greater susceptibility to stress when low nutrient availability is combined with reduced blue light, resulting in

Table 6: Concentration of sucrose (mg g^{-1} FW) in lettuce leaves after the first and second harvest, and after storage. The data represents the average for each treatment ± the standard error. Letters indicate significant differences between the combinations of light and EC according to Tukey's post-hoc test where treatments sharing at least one letter are not significantly different. Effects of electrical conductivity (EC), blue light proportion (% blue), and their interaction for each harvest through the two-way ANOVA testing (bottom panel). Significance levels are indicated as ns ($p > 0.05$), * ($p < 0.05$), and *** ($p < 0.001$).

EC [dS m^{-1}]	% blue	first harvest	second harvest	storage
1	high	7.62 ± 0.23 a	6.60 ± 0.50 a	3.82 ± 1.12 a
1	variable	5.72 ± 1.30 abc	6.55 ± 0.73 a	2.34 ± 0.44 ab
1	low	6.52 ± 0.54 ab	4.36 ± 0.99 ab	1.85 ± 0.69 ab
2	high	2.38 ± 0.81 c	2.53 ± 0.78 b	1.19 ± 0.36 b
2	variable	4.77 ± 0.71 abc	2.47 ± 0.91 b	1.04 ± 0.25 b
2	low	5.51 ± 1.16 abc	4.38 ± 0.68 ab	1.09 ± 0.20 b
3	high	2.67 ± 0.79 bc	2.37 ± 0.48 b	0.54 ± 0.07 b
3	variable	3.23 ± 0.95 bc	1.84 ± 0.16 b	0.64 ± 0.13 b
3	low	3.62 ± 0.34 bc	2.18 ± 0.64 b	0.80 ± 0.31 b
% blue combined with EC		ns	*	ns
% blue		ns	ns	ns
EC		***	***	***

weaker protective responses and higher membrane permeability. Light spectrum has been shown to affect membrane integrity in lettuce, with different Red:Blue ratios influencing EL and drought tolerance [44].

After storage, EL increased slightly with increasing EC in plants grown under high blue light, rising from 9.1% to 13.8% (Fig. 8 C).

3.2 Outcomes of the hyperspectral data analysis

In this section, we report the main outcomes of the hyperspectral data analysis. First, we assessed whether spectral data could discriminate between freshly harvested and stored leaves through a classification task. Second, we identified the spectral regions that contributed most to the separation between classes. Finally, we explored the relationships between spectral indices and chemical traits to identify potential non-destructive indicators of postharvest biochemical changes.

3.2.1 Classification of post-harvest stages

The classification results confirmed that hyperspectral reflectance contains sufficient information to discriminate between freshly harvested and stored lettuce leaves. Among

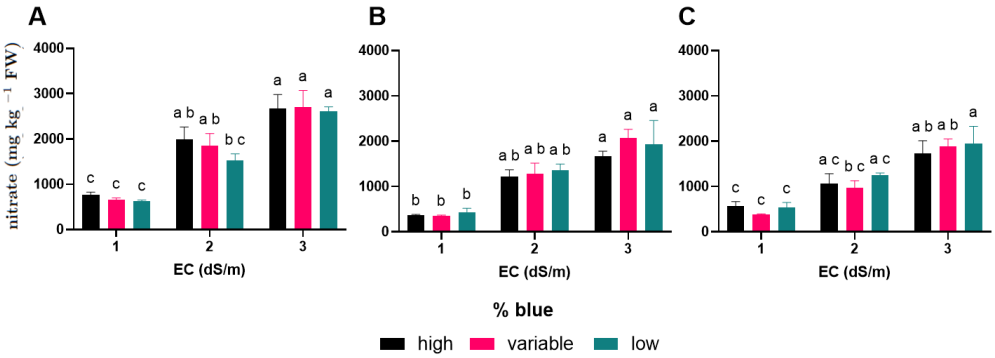

Figure 7: Nitrate concentration (mg kg^{-1} FW) in lettuce leaves after the first (A), second (B) harvest, and after the storage (C).The data represents the average for each treatment ± the standard error. Letters indicate significant differences between the combinations of light and EC according to Tukey's post-hoc test where treatments sharing at least one letter are not significantly different.

the tested preprocessing and feature-reduction strategies, the best-performing configuration combined standard normal variate transformation with the first 10 principal components, achieving a test-set accuracy of 0.88 (i.e., the proportion of correctly classified samples). These findings indicate that storage-induced changes in leaf properties are captured by spectral signatures, supporting the use of hyperspectral imaging for postharvest quality monitoring.

3.2.2 Spectral regions contributing to class separation

To highlight which wavelengths drove the separation between stages, we examined the contribution of the original features to the two XGBoost-most relevant principal components, PC1 and PC4. Two regions emerged as most influential (see Figure 9): (i) 580–616 nm, where chlorophyll loss increases reflectance [45]; (ii) 670–715 nm, a region known to be sensitive to water content [46]. These findings align with established post-harvest physiology, in which early pigment degradation and red-edge shifts signal deterioration [46].

3.2.3 Spectral indices as indicators of chemical variation

We also evaluated whether spectral indices computed from the Δ-spectra of each growing condition reflected the corresponding changes in chemical traits. Because the dataset included only nine growing conditions, regression analyses would be underpowered. Therefore, this step was intended as exploratory rather than causal. The objective was to identify candidate spectral indices that may act as non-destructive indicators of postharvest chemical shifts and could be tested in larger, multi-batch experiments to support future predictive models. To this end, Pearson correlation coefficients were computed for each

Table 7: Total anthocyanin (Cyanidin eq. mg g^{-1} FW) in lettuce leaves after the first and second harvest, and after storage (top panel). The data represents the average for each treatment ± the standard error. Letters indicate significant differences between the combinations of light and EC according to Tukey's post-hoc test where treatments sharing at least one letter are not significantly different. Effects of electrical conductivity (EC), blue light proportion (% blue), and their interaction for each harvest through the two-way ANOVA testing (bottom panel). Significance levels are indicated as ns ($p > 0.05$), * ($p < 0.05$), ** ($p < 0.01$), and *** ($p < 0.001$).

EC [dS m^{-1}]	% blue	first harvest	second harvest	storage
1	high	34.8 ± 5.20 abc	39.9 ± 7.32 a	38.5 ± 3.13 a
1	variable	40 ± 3.41 a	28.7 ± 8.90 ab	33.6 ± 3.47 ab
1	low	26.6 ± 2.12 abc	20 ± 4.01 ab	34.7 ± 6.82 ab
2	high	22.1 ± 5.04 bc	17.7 ± 2.39 b	20.4 ± 2.09 bc
2	variable	28.1 ± 2.46 abc	9.6 ± 1.22 b	26.7 ± 2.08 abc
2	low	19.5 ± 3.24 c	14.3 ± 2.20 b	21.9 ± 3.70 bc
3	high	36.6 ± 3.91 ab	11.2 ± 1.96 b	15.8 ± 0.32 c
3	variable	22.7 ± 2.22 bc	13.6 ± 2.06 b	17.5 ± 1.81 c
3	low	20.6 ± 1.24 bc	17.3 ± 2.46 b	16.3 ± 1.82 c
% blue combined with EC		*	ns	ns
% blue		**	ns	ns
EC		**	***	***

index–trait pair. As shown in Fig. 10, for most chemical traits one or two indices displayed strong associations (Pearson $r > 0.6$). Moreover, the consistency of correlations for traits expressed on both fresh- and dry-weight bases supports the robustness and biological relevance of the identified indices.

Total anthocyanins and phenolic index NDRE showed strong negative correlations with both anthocyanins and the phenolic index, consistent with its sensitivity to red-edge shifts that can be driven not only by chlorophyll but also by broader changes in the pigment pool [47, 48]. $NDWI_{970}$ was strongly and positively associated with anthocyanins and the phenolic index. Although $NDWI_{970}$ is primarily linked to leaf-water absorption near 970 nm [49], water content in our dataset remained stable or slightly decreased from harvest to storage, suggesting that this relationship is unlikely to reflect a direct physiological coupling between water status and anthocyanin accumulation. Instead, the correlation may arise from indirect structural and optical effects, as changes in pigment distribution can influence reflectance near the NIR–SWIR transition independently of leaf water content [50].

GNDVI exhibited moderate negative correlations with anthocyanins, consistent with its interpretation as a greenness index. Because anthocyanins absorb in the green region (500–600 nm), increasing anthocyanin concentration reduces apparent greenness and

Table 8: Phenol index (ABS_{320} nm g^{-1} FW) in lettuce leaves after the first and second harvest, and after storage (top panel). The data represents the average for each treatment ± the standard error. Letters indicate significant differences between the combinations of light and EC according to Tukey's post-hoc test where treatments sharing at least one letter are not significantly different. Effects of electrical conductivity (EC), blue light proportion (% blue), and their interaction for each harvest through the two-way ANOVA testing (bottom panel). Significance levels are indicated as ns ($p > 0.05$), * ($p < 0.05$), ** ($p < 0.01$), and *** ($p < 0.001$).

EC [dS m^{-1}]	% blue	I harvest	II harvest	Storage
1	high	60.8 ± 7.78 a	56.8 ± 6.17 ab	62.4 ± 5.45 a
1	variable	59.7 ± 5.33 a	61.1 ± 10.14 a	51.7 ± 3.83 abc
1	low	41.4 ± 5.58 abc	29.0 ± 9.37 bc	52.5 ± 8.76 ab
2	high	30.5 ± 7.65 bc	16.2 ± 3.62 c	24.1 ± 1.09 d
2	variable	41.1 ± 3.40 abc	7.4 ± 2.82 c	34.4 ± 4.63 bcd
2	low	28.2 ± 6.11 bc	13.1 ± 4.71 c	29.9 ± 6.60 cd
3	high	53.2 ± 4.48 ab	5.6 ± 1.36 c	16.1 ± 0.74 d
3	variable	25.1 ± 2.59 c	10.1 ± 4.58 c	18.5 ± 1.35 d
3	low	23.8 ± 3.27 c	14.5 ± 5.30 c	17.4 ± 2.06 d
% blue combined with EC		*	*	ns
% blue		**	ns	ns
EC		***	***	***

therefore decreases GNDVI [45, 51]. Notably, ARI1, an index originally proposed to track anthocyanin accumulation [52, 51], showed unexpectedly weak correlations with measured anthocyanins in this dataset. Instead, ARI1 was more strongly associated with sugar-related traits.

Chlorophylls As expected, NDRE was strongly and negatively correlated with chlorophyll content [53], with a stronger association for chlorophyll *b* than for chlorophyll *a*. This is physiologically plausible because chlorophyll *a* absorbs maximally at 662 nm, whereas chlorophyll *b* absorbs at 642–650 nm [54]. The closer proximity of chlorophyll *b* absorption to the red-edge region makes it particularly influential in shaping the slope and position of the red-edge. PRI showed consistently positive correlations with all chlorophyll metrics, in agreement with its established use as a proxy for light-use efficiency [55, 56]. Leaves with higher chlorophyll content typically exhibit greater photosynthetic capacity and improved regulation of absorbed light energy [57]. WBI also correlated positively with chlorophylls, especially when traits were expressed on a dry-weight basis. Because WBI is primarily a water-related index [58], the stronger association for dry-weight-normalized data may indicate that, once bulk water content is accounted for, co-variation between pigment accumulation and leaf hydration becomes more apparent [50, 59].

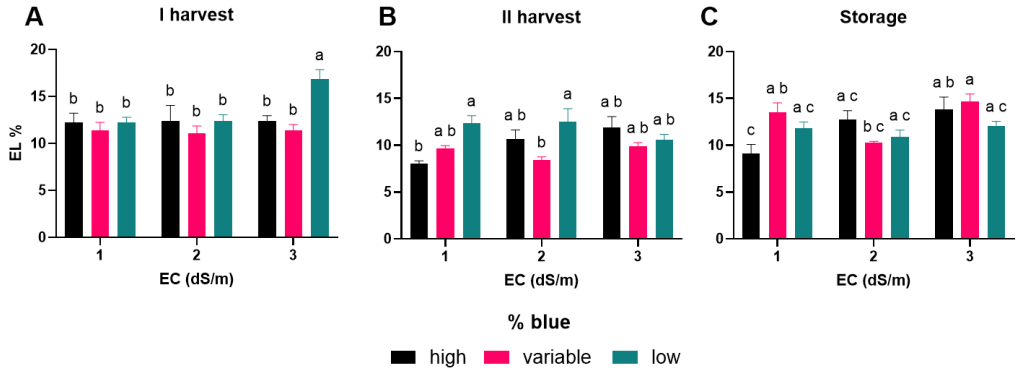

Figure 8: Electrolyte leakage (%) in lettuce leaves after the first (A), second (B) harvest, and after the storage (C). The data represents the average for each treatment ± the standard error. Letters indicate significant differences between the combinations of light and EC according to Tukey's post-hoc test where treatments sharing at least one letter are not significantly different.

Carotenoids Correlations with carotenoids alone were generally weaker. NDRE showed moderate negative correlations, consistent with increased absorption in the red region as the overall pigment pool rises. CRI1, which was developed to track carotenoid variation by leveraging absorption features around 500–550 nm [60], displayed only a slight negative association. Stronger relationships emerged when pigment ratios were considered: the senescence-sensitive Car/Chl ratio [60] was strongly correlated with PSRI, in line with the theoretical formulation of PSRI and its validation as an indicator of senescence-related pigment shifts [48].

Nitrate PSRI showed moderate positive correlations with nitrate content, consistent with the idea that senescence-related changes (higher PSRI) are associated with reduced nitrate assimilation and, consequently, higher residual nitrate in the tissue. In contrast, NDRE and GNDVI were negatively correlated with nitrates, suggesting that greener and more photosynthetically active leaves assimilate nitrate more efficiently, resulting in lower residual concentrations. Notably, although CRI1 was developed to track carotenoids, it displayed negative correlations with nitrates, which may reflect indirect co-variation between nitrogen status and pigment composition.

Total sugars, reducing sugars, and sucrose Sugar-related patterns were among the most distinctive. GNDVI showed strong positive correlations with total sugars, indicating that greenness co-varies with carbohydrate pools, as leaves with higher chlorophyll content and photosynthetic capacity tend to accumulate more carbohydrates [51]. In contrast, PSRI was strongly and negatively correlated with all sugar traits, consistent with its interpretation as a senescence index: higher PSRI values are associated with older, less photosynthetically active tissues and therefore lower carbohydrate contents

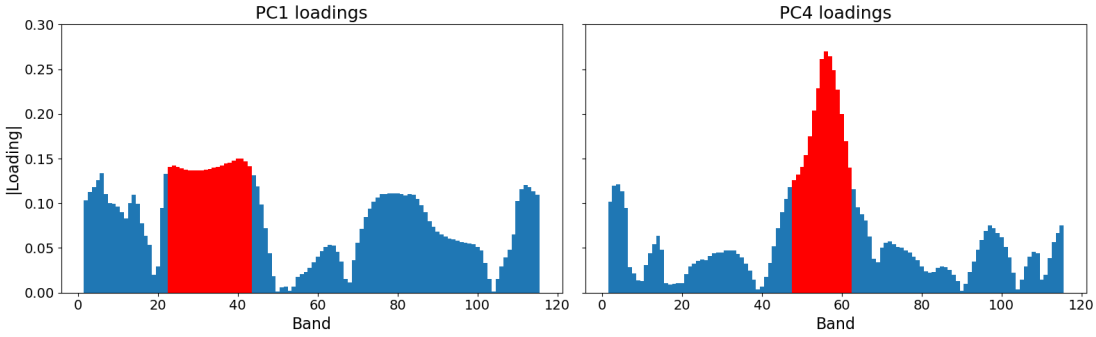

Figure 9: Loadings of the original spectral bands on the two most influential principal components (PC1 and PC4) according to the XGBoost classifier, as a function of the band number. The bands with the strongest contributions to each component are red-highlighted. Notice that the conversion from band number to wavelength follows a linear relation, as the camera acquires 120 evenly spaced bands between 400 and 1000 nm.

[48, 60]. ARI1 also correlated strongly and positively with sugars, particularly reducing sugars. Although ARI1 was originally developed for anthocyanin detection, it was only weakly associated with anthocyanins in this dataset; therefore, the observed association with sugars likely reflects shared co-variation with chlorophyll and overall leaf physiological status. BNDVI showed strong negative correlations with total sugars, potentially because absorption in the blue region (around 450 nm) is influenced by phenolics and anthocyanins, which can covary with carbohydrate metabolism [50, 52]. Finally, NDVI showed mixed associations: it was weakly negative with total sugars (r about -0.3) but positive with reducing sugars (r about 0.5), suggesting that NDVI may track photosynthetic activity more closely (linked to reducing sugars as immediate photosynthates) than longer-term carbohydrate storage [47].

4 Conclusions

This study shows that both nutrient-solution dilution (EC) and blue-light proportion influence the growth and quality of lettuce cultivated in a vertical farming system, and that their interaction contributes to shaping several responses. Higher EC accelerated growth, although this did not consistently translate into higher yield, while blue light modulated plant compactness. Across sampling times, clear treatment-dependent differences emerged for total sugars, reducing sugars, and nitrate concentration, highlighting trade-offs between carbohydrate accumulation and nitrate content under contrasting EC–light combinations.

Table 9 provides an overview of the correlation results between vegetation indices and biochemical traits. Among these, the most consistent and physiologically interpretable ones were: (i) NDRE strongly negative with anthocyanins and chlorophylls; (ii) PRI positive with chlorophylls; (iii) NDWI_{970} strongly positive with the anthocyanins

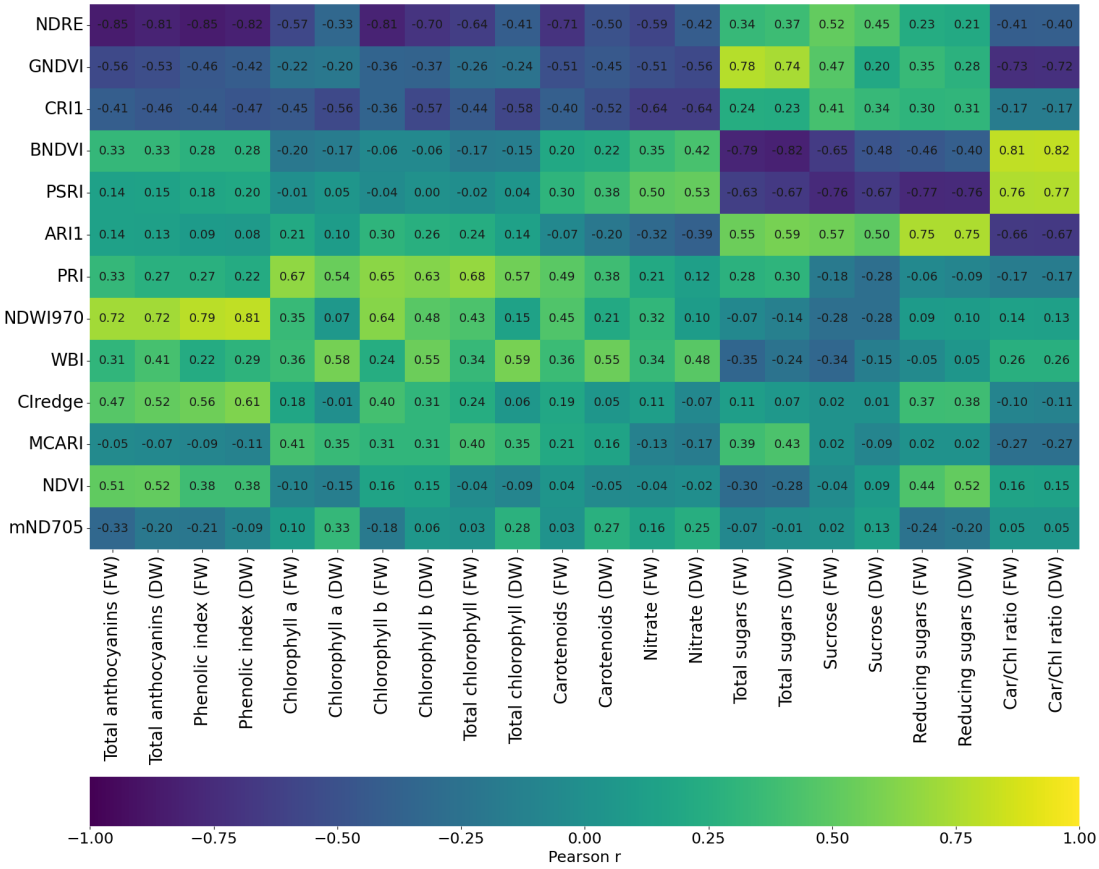

Figure 10: Heatmap of Pearson correlation coefficients between spectral indices and chemical traits across treatments. Positive values indicate that increases in an index are associated with increases in the corresponding trait, and vice versa. Values are reported for both fresh weight (FW) and dry weight (DW) measurements.

and phenolic index; (iv) PSRI strongly negative with sugars and strongly positive with carotenoid-to-chlorophyll ratio; (v) ARI1 strongly positive with sugars (particularly reducing sugars) and strongly negative with carotenoid-to-chlorophyll ratio; (vi) GNDVI strongly positive with total sugars and strongly negative with carotenoid-to-chlorophyll ratio. These findings are consistent with the established spectral sensitivity of vegetation indices but also reveal dataset-specific co-variations, such as the parallel increase of anthocyanins with water-related indices. The differentiation between chlorophyll *a* and *b* correlations with red-edge indices further highlights the spectral-physiological specificity of light-harvesting pigments. Finally, it is worth noting that WBI also correlated positively with chlorophylls, especially in DW data, possibly reflecting co-variation between pigment concentration and mesophyll hydration, suggesting that this index may provide

complementary structural information beyond its established role as a water-related indicator.

Table 9: Overview of the most relevant correlations between vegetation indices and biochemical traits, with arrow directions reflecting the sign of the Pearson correlation coefficient.

Index	**Main correlated traits**	**Interpretation**
NDRE	↓ Chlorophylls (especially Chlorophylls *b*), Anthocyanins, Phenolic index, Carotenoids	Sensitive to red-edge shifts due to total pigment content
PRI	↑ Chlorophylls	Proxy for light-use efficiency and xanthophyll cycle
$NDWI_{970}$	↑ Anthocyanins, Phenolic index	Links pigment accumulation with mesophyll hydration
PSRI	↓ Sugars, ↑ Car/Chl	Marker of senescence
ARI1	↑ Sugars (especially reducing sugars), ↓ Car/Chl	Reflects anthocyanin–sugar co-regulation and N–pigment imbalance
GNDVI	↑ Total sugars, ↓ Car/Chl	Greenness relates to carbohydrate pools, decreases with senescence
WBI	↑ Chlorophylls (especially DW)	Co-variation of pigments and mesophyll water content
BNDVI	↓ Sugars, ↑ Car/Chl	Blue absorption by phenolics/anthocyanins linked to sugar metabolism
NDVI	↑ Reducing sugars, ↓ Total sugars	Tracks immediate photosynthetic activity versus carbohydrate storage

5 Data availability statement

The experimental data not explicitly reported in this paper, as well as the collected images, are not publicly available. These data are subject to confidentiality restrictions at the request of Agricola Moderna, which hosted the experimental activities. Access may be granted upon request and with permission from Agricola Moderna.

6 Credits

Giulia Franzoni: Data curation, Formal analysis, Investigation, Writing- Original draft preparation , Susanna Mirabella: Data curation, Formal analysis, Investigation, Writing- Original draft preparation, Aleksander Dabek: Data curation, Formal analysis, Investigation, Writing- Original draft preparation, Nicola Ferro: Supervision, Writing- review and editing, Alessandro Antona: Formal anlaysis, Resources and methodology, Writing- review and editing , Martina Carlessi: Formal anlaysis, Resources and methodology, Simone Cinquemani: Conceptualization, supervision, Writing- review and editing, Matteo Matteucci: Conceptualization, Supervision, Writing- review and editing, Giacomo Cocetta: Conceptualization, Supervision, Writing- review and editing, Simona Perotto: Conceptualization, supervision, writing-review and editing

References

[1] T. Kozai, G. Niu, and M. Takagaki, editors. *Plant Factory: An Indoor Vertical Farming System for Efficient Quality Food Production.* Academic Press, 2 edition, 2019.

[2] K. R. Cope and B. Bugbee. Spectral effects of three types of white light-emitting diodes on plant growth and development: absolute versus relative amounts of blue light. *HortScience*, 48(4):504–509, 2013.

[3] C. Fallovo, Y. Rouphael, E. Rea, A. Battistelli, and G. Colla. Nutrient solution concentration and growing season affect yield and quality of Lactuca sativa L. var. acephala in floating raft culture. *Journal of the Science of Food and Agriculture*, 89(10):1682–1689, 2009.

[4] Z. Ye, X. Tan, M. Dai, X. Chen, Y. Zhong, Y. Zhang, Yu. Ruan, and D. Kong. A hyperspectral deep learning attention model for predicting lettuce chlorophyll content. *Plant Methods*, 20(1):22, 2024.

[5] S. Yu, J. Fan, X. Lu, W. Wen, S. Shao, X. Guo, and C. Zhao. Hyperspectral technique combined with deep learning algorithm for prediction of phenotyping traits in lettuce. *Frontiers in Plant Science*, 13:927832, 2022.

[6] H. K. Lichtenthaler. Chlorophylls and carotenoids: pigments of photosynthetic biomembranes. *Methods in Enzymology*, 148:350–382, 1987.

[7] E. W. Yemm and A. Willis. The estimation of carbohydrates in plant extracts by anthrone. *Biochemical Journal*, 57(3):508, 1954.

[8] G. L. Miller. Use of dinitrosalicylic acid reagent for determination of reducing sugar. *Analytical Chemistry*, 31(3):426–428, 1959.

[9] E. S. Rorem, H. G. Walker, and R. M. McCready. Biosynthesis of sucrose and sucrose-phosphate by sugar beet leaf extracts. *Plant Physiology*, 35(2):269, 1960.

[10] D. A. Cataldo, M. Maroon, L. E. Schrader, and V. L. Youngs. Rapid colorimetric determination of nitrate in plant tissue by nitration of salicylic acid. *Communications in Soil Science and Plant Analysis*, 6(1):71–80, 1975.

[11] D. Ke and M. E. Saltveit. Wound-induced ethylene production, phenolic metabolism and susceptibility to russet spotting in iceberg lettuce. *Physiologia Plantarum*, 76(3):412–418, 1989.

[12] A. O. Klein and C. W. Hagen. Anthocyanin production in detached petals of impatiens balsamina L. *Plant Physiology*, 36(1):1, 1961.

[13] J. G. Kim, Y. Luo, R. A. Saftner, and K. C. Gross. Delayed modified atmosphere packaging of fresh-cut romaine lettuce: Effects on quality maintenance and shelf-life. *Journal of the American Society for Horticultural Science*, 130(1):116–123, 2005.

[14] A. A. Gitelson, Y. J. Kaufman, and M. N. Merzlyak. Use of a green channel in remote sensing of global vegetation from eos-modis. *Remote Sensing of Environment*, 58:289–298, 1996.

[15] J. A. Gamon, J. Peñuelas, and C. B. Field. A narrow-waveband spectral index that tracks diurnal changes in photosynthetic efficiency. *Remote Sensing of Environment*, 41:35–44, 1992.

[16] D. A. Sims and J. A. Gamon. Relationships between leaf pigment content and spectral reflectance across a wide range of species, leaf structures and developmental stages. *Remote Sensing of Environment*, 81:337–354, 2002.

[17] Anatoly A Gitelson, Mark N Merzlyak, and Olga B Chivkunova. Optical properties and nondestructive estimation of anthocyanin content in plant leaves¶. *Photochemistry and photobiology*, 74(1):38–45, 2001.

[18] C. S. T. Daughtry, C. L. Walthall, M. S. Kim, E. B. De Colstoun, and J. E. McMurtrey. Estimating corn leaf chlorophyll concentration from leaf and canopy reflectance. *Remote Sensing of Environment*, 74:229–239, 2000.

[19] Xavier A. Jaime, Jay P. Angerer, Chenghai Yang, Douglas R. Tolleson, Samuel D. Fuhlendorf, and X. Ben Wu. Effects of prescribed fire on spatial patterns of plant functional traits and spectral diversity using hyperspectral imagery from savannah landscapes on the edwards plateau of texas, usa. *Remote Sensing*, 17(23):3873, 2025.

[20] J. Traba, J. Gómez-Catasús, A. Barrero, D. Bustillo-de la Rosa, J. Zurdo, I. Hervás, C. Pérez-Granados, E. L. García de la Morena, A. Santamaría, and M. Reverter. Comparative assessment of satellite- and drone-based vegetation indices to predict arthropod biomass in shrub-steppes. *Ecological Applications*, 32(8):e2707, 2022.

[21] K.L. Castro-Esau, G.A. Sánchez-Azofeifa, and B. Rivard. Comparison of spectral indices obtained using multiple spectroradiometers. *Remote Sensing of Environment*, 103(3):276–288, 2006. Spectral Network.

[22] Bo cai Gao. Ndwi—a normalized difference water index for remote sensing of vegetation liquid water from space. *Remote Sensing of Environment*, 58(3):257–266, 1996.

[23] D. M. Kim, H. Zhang, H. Zhou, T. Du, Q. Wu, T. C. Mockler, and M. Y. Berezin. Highly sensitive image-derived indices of water-stressed plants using hyperspectral imaging in swir and histogram analysis. *Scientific Reports*, 5:15919, 2015.

[24] D. B. Egli. Time and the productivity of agronomic crops and cropping systems. *Agronomy Journal*, 103(3):743–750, 2011.

[25] J. S. Matthews, S. Vialet-Chabrand, and T. Lawson. Role of blue and red light in stomatal dynamic behaviour. *Journal of Experimental Botany*, 71(7):2253–2269, 2020.

[26] W. L. Sublett, T. C. Barickman, and C. E. Sams. The effect of environment and nutrients on hydroponic lettuce yield, quality, and phytonutrients. *Horticulturae*, 4(4):48, 2018.

[27] E. Quattrini, M. Penati, A. Alberici, L. Martinetti, P. Marino Gallina, A. Ferrante, and M. Schiavi. Effect of the reduction of nutrient solution concentration on leafy vegetables quality grown in floating system. In *International Symposium on High Technology for Greenhouse System Management: Greensys2007*, volume 801, pages 1167–1176. International Society for Horticultural Science, 2007.

[28] S. E. Wortman. Crop physiological response to nutrient solution electrical conductivity and pH in an ebb-and-flow hydroponic system. *Scientia Horticulturae*, 194:34–42, 2015.

[29] X.-L. Chen, L.-C. Wang, T. Li, Q.-C. Yang, and W.-Z. Guo. Sugar accumulation and growth of lettuce exposed to different lighting modes of red and blue led light. *Scientific Reports*, 9:6926, 2019.

[30] K. H. Son, J. H. Lee, Y. Oh, D. Kim, M. M. Oh, and B. C. In. Growth and bioactive compound synthesis in cultivated lettuce subject to light-quality changes. *HortScience*, 52(4):584–591, 2017.

[31] M. Lee, J. Xu, W. Wang, and C. B. Rajashekar. The effect of supplemental blue, red and far-red light on the growth and the nutritional quality of red and green leaf lettuce. *American Journal of Plant Sciences*, 10(12):2219–2235, 2019.

[32] J. Song, H. Huang, Y. Hao, S. Song, Y. Zhang, W. Su, and H. Liu. Nutritional quality, mineral and antioxidant content in lettuce affected by interaction of light intensity and nutrient solution concentration. *Scientific Reports*, 10:2796, 2020.

[33] J. Wang, W. Lu, Y. Tong, and Q. Yang. Leaf morphology, photosynthetic performance, chlorophyll fluorescence, stomatal development of lettuce (Lactuca sativa L.) exposed to different ratios of red light to blue light. *Frontiers in Plant Science*, 7:250, 2016.

[34] X.-L. Chen, Y.L. Li, L.-C. Wang, and W.-Z. Guo. Red and blue wavelengths affect the morphology, energy use efficiency and nutritional content of lettuce (Lactuca sativa L.). *Scientific Reports*, 11:8374, 2021.

[35] M. P. Gent. Solution electrical conductivity and ratio of nitrate to other nutrients affect accumulation of nitrate in hydroponic lettuce. *HortScience*, 38(2):222–227, 2003.

[36] N. Van Quy, W. Sinsiri, S. Chitchamnong, K. Boontiang, and W. Kaewduangta. Effects of electrical conductivity (EC) of the nutrient solution on growth, yield and quality of lettuce under vertical hydroponic systems. *Khon Kaen Agricultural Journal*, 46(3):613–622, 2018.

[37] A. Signore, L. Bell, P. Santamaria, C. Wagstaff, and M. C. Van Labeke. Red light is effective in reducing nitrate concentration in rocket by increasing nitrate reductase activity, and contributes to increased total glucosinolates content. *Frontiers in Plant Science*, 11:604, 2020.

[38] Cathrine Lillo. Light regulation of nitrate uptake, assimilation and metabolism. In Sara Amâncio and Ineke Stulen, editors, *Nitrogen Acquisition and Assimilation in Higher Plants*, pages 149–184. Springer Netherlands, Dordrecht, 2004.

[39] R. Akula and G. A. Ravishankar. Influence of abiotic stress signals on secondary metabolites in plants. *Plant Signaling Behavior*, 6(11):1720–1731, 2011.

[40] K. Shoji, E. Goto, S.-N. Hashida, F. Goto, and T. Yoshihara. Effect of red light and blue light on the anthocyanin accumulation and expression of anthocyanin biosynthesis genes in red-leaf lettuce. *Shokubutsu Kankyo Kogaku*, 22(2):107–113, 2010.

[41] Y. Li, L. Wu, H. Jiang, R. He, S. Song, W. Su, and H. Liu. Supplementary far-red and blue lights influence the biomass and phytochemical profiles of two lettuce cultivars in plant factory. *Molecules*, 26(23):7405, 2021.

[42] C. Kaya, D. Higgs, and E. Sakar. Response of two leafy vegetables grown at high salinity to supplementary potassium and phosphorus during different growth stages. *Journal of Plant Nutrition*, 25(12):2663–2676, 2002.

[43] G. Kaya. Ameliorative effects of foliar potassium nitrate on the growth, physiological, and stomatal properties of lettuce plants under salinity stress. *Journal of Plant Nutrition*, 46(12):2882–2892, 2023.

[44] D. N. Ginzburg and J. D. Klein. Led pre-exposure shines a new light on drought tolerance complexity in lettuce (Lactuca sativa) and rocket (Eruca sativa). *Environmental and Experimental Botany*, 180:104240, 2020.

[45] A. A. Gitelson, Y. J. Kaufman, and M. N. Merzlyak. Use of a green channel in remote sensing of global vegetation from eos-modis. *Journal of Plant Physiology*, 148(3–4):494–500, 1996.

[46] B. Diezma, L. Lleó, J. M. Roger, A. Herrero-Langreo, L. Lunadei, and M. Ruiz-Altisent. Examination of the quality of spinach leaves using hyperspectral imaging. *Postharvest Biology and Technology*, 85:8–17, 2013.

[47] A. A. Gitelson and M. N. Merzlyak. Spectral reflectance changes associated with autumn senescence of Aesculus hippocastanum L. and Acer platanoides L. leaves. *Remote Sensing of Environment*, 48(3):213–222, 1994.

[48] M. N. Merzlyak, A. A. Gitelson, O. B. Chivkunova, and V. Yu. Rakitin. Non-destructive optical detection of leaf senescence. *Physiologia Plantarum*, 106(1):135–141, 1999.

[49] B.-C. Gao. NDWI—A normalized difference water index for remote sensing of vegetation liquid water. *Remote Sensing of Environment*, 58(3):257–266, 1996.

[50] G. A. Carter and A. K. Knapp. Leaf optical properties in higher plants: linking spectral characteristics to stress and chlorophyll concentration. *Photosynthesis Research*, 67(1):1–10, 2001.

[51] D. A. Sims and J. A. Gamon. Relationships between leaf pigment content and spectral reflectance across a wide range of species, leaf structures and developmental stages. *Remote Sensing of Environment*, 81(2–3):337–354, 2002.

[52] A. A. Gitelson, Y. Zur, O. B. Chivkunova, and M. N. Merzlyak. Optical remote estimation of chlorophyll, carotenoid and anthocyanin contents in higher plant leaves. *Remote Sensing of Environment*, 77(2):274–281, 2001.

[53] A. A. Gitelson, Y. Gritz, and M. N. Merzlyak. Relationships between leaf chlorophyll content and spectral reflectance and algorithms for non-destructive chlorophyll assessment in higher plant leaves. *Journal of Plant Physiology*, 160(3):271–282, 2003.

[54] H. K. Lichtenthaler and C. Buschmann. Chlorophylls and carotenoids: Measurement and characterization by UV-VIS spectroscopy. *Photosynthetica*, 43(3):352–369, 2001.

[55] J. A. Gamon, J. Peñuelas, and C. B. Field. A narrow-waveband spectral index that tracks diurnal changes in photosynthetic efficiency. *Remote Sensing of Environment*, 41(1):35–44, 1992.

[56] M. F. Garbulsky, J. Peñuelas, D. Papale, and I. Filella. The photochemical reflectance index (PRI) and the remote sensing of photosynthetic light use efficiency: A review and meta-analysis. *Remote Sensing of Environment*, 115(2):281–297, 2011.

[57] J. R. Evans. Photosynthesis and nitrogen relationships in leaves of C3 plants. *Oecologia*, 78:9–19, 1989.

[58] J. Peñuelas and I. Filella. Visible and near-infrared reflectance techniques for diagnosing plant physiological status. *Trends in Plant Science*, 2(8):287–291, 1997.

[59] S. Jacquemoud and S. L. Ustin. *Leaf Optical Properties*. Cambridge University Press, 2019.

[60] A. A. Gitelson, Y. Zur, O. B. Chivkunova, and M. N. Merzlyak. Assessing carotenoid content in plant leaves with reflectance spectroscopy. *Journal of Experimental Botany*, 53(372):1359–1369, 2002.

MOX Technical Reports, last issues

Dipartimento di Matematica
Politecnico di Milano, Via Bonardi 9 - 20133 Milano (Italy)

Franzoni, G.; Mirabella, S.; Dabek, A.; Ferro, N.; Antona, A.; Carlessi, M.; Cinquemani, S.; Matteucci, M.; Cocetta, G.; Perotto, S.
ntegrating Environmental Control and Hyperspectral Imaging to Assess Light and Nutrient Effects on Lettuce Post-Harvest Quality in Vertical Farming

32/2026 Antonietti, P.F.; Bonizzoni, F.; Perugia, I.; Verani, M.
A Multilevel Monte Carlo Virtual Element Method for Uncertainty Quantification of Elliptic Partial Differential Equations

31/2026 Guastamacchia, C.; Piersanti, R; Giardini, F.; Coppini, R.; Ferrantini C.; Dede' L.; Sacconi L.; Regazzoni F.
The functional impact of myofiber macroscopic organization and disarray in computational models of the murine heart

30/2026 Regazzoni, F.
The internal law of a material can be discovered from its boundary

28/2026 Daniele, F.; Leimer Saglio, C. B.; Pagani, S.; Antonietti, P. F.
Mathematical and numerical modeling of coupled oxygen dynamics and neuronal electrophysiology

27/2026 Antonietti, P. F.; Abdalla, O. M. O.; Garroni, M. G.; Mazzieri, I.; Parolini, N.
A hybrid reduced-order and high-fidelity discontinuous Galerkin Spectral Element framework for large-scale PMUT array simulations

23/2026 Ballini, E.; Muscarnera, L.; Fumagalli, A.; Scotti, A.; Regazzoni, F.
Elimination-compensation pruning for fully-connected neural networks

26/2026 Dokuchaev, A.; Bonizzoni, F.; Pagani, S.; Regazzoni, F.; Pezzuto, S.
Learning geometry-dependent lead-field operators for forward ECG modeling

25/2026 Carrara, D.; Hirschvogel, M.; Bonizzoni, F.; Pagani, S.; Pezzuto, S.; Regazzoni, F.
Shape-informed cardiac mechanics surrogates in data-scarce regimes via geometric encoding and generative augmentation

21/2026 Bottacini, G.; Torzoni, M.; Manzoni, A.
Neural Markov chain Monte Carlo: Bayesian inversion via normalizing flows and variational autoencoders